Shape Retrieval Using Eigen and Fisher Barycenter Contour

Kosorl Thourn[1], **Yuttana Kitjaidure**[2], and **Shozo Kondo**[3], Non-members

ABSTRACT

To achieve a good performance for shape retrieval, it requires both shape representation and classifier. In this paper, the algorithm for shape matching and retrieval is developed by using Eigen Barycenter Contour (EBcC) and Fisher Barycenter Contour (FBcC). In our algorithm, the Signed Enclosed Area (SEA) signature (formed by two adjacent points of contour and its center point), computed at each scale level of Barycenter contour (BcC), is utilized as the shape representation. The BcC technique is robust to moderate amount of noise and occlusion. Furthermore, the SEA signature is invariant to general affine transformation including translation, rotation, scale and shear. Because of high dimension of the shape representation, thus, in the matching step, two classifiers have been studied. The first classifier, Eigen face technique, is employed for dimensionality reduction while the second classifier, Fisher face technique, is used for reducing dimension as well and making discrimination. Then, the similarity among shapes is measured by the normalized cross-correlation (NCC). The performance of our technique is evaluated onto the affine shape database and two well-known databases, the MPEG-7 shape database part B and the Kimia's database. The experimental results illustrate that our approach gives very high retrieval efficiency over all published methods.

Keywords: Affine Transformation, Barycenter Contour (BcC), Invariant to Starting Point, Eigen Barycenter Contour (EBcC), Fisher Barycenter Contour (FBcC), Normalized Cross Correlation (NCC).

1. INTRODUCTION

In computer vision area, several algorithms or computer program have been developed for artificial vision. Such a wide range of algorithms is not only utilized for computer but also robot and other machines for their artificial vision which provides an ease for life and is important for industrial applications and others.

Several properties, obtained from the objects, have been used for recognition and categorization such as shape, colour, texture, brightness, and others. Of such properties, human can easily recognize and identify a type of the objects using their geometries (shape) rather than intensities (colour, texture, brightness). That is why shape has been considered as an important visual feature and as the most promising in a system for object recognition, matching, registration, and analysis. In addition, the users are interested in retrieval by shape rather than by the others as indicated in [1].

In our previous work [2], BcC was utilized to decompose the shape contour into multi-scale levels. Then, SEA is computed at each scale level of BcC for shape representation. The algorithm has been done in the frequency domain to be invariant to starting point selection and the matching based on Principle Component Analysis (PCA) is tested for the affine shape database.

In this paper, we develop the algorithm for 2D shape matching to improve the retrieval performance using Fisher Discriminant Analysis (FDA) in the frequency domain as well. A comparison study between both classifier, PCA and FDA is done in this literature.

The paper is organized as follows: Section 2 gives a review of the previous techniques. The proposed method is introduced in section 3 followed by the feature extraction in section 4 (Boundary extraction, Barycenter contour decomposition, and Shape representation). Then, shape matching is given in section 5. Next, the experimental results are illustrated in section 6. Finally, conclusion is given in section 7.

2. PREVIOUS WORKS

Several techniques of shape matching and retrieval for 2D closed boundary shape have been developed over the past decade. Good review papers can be found in [3]. However, we focus our review on the multi-scale representations (for example curvature scale space CSS, wavelet) and the classification based on the eigen techniques [4, 5].

El Rube et al. [6] have proposed a zero crossing of the triangle area representation (TAR) at multi-scale wavelet levels (called MTAR) to construct MTAR image. First, the wavelet transform is used

Manuscript received on August 1, 2009 ; revised on December 21, 2009.

[1,2] The authors are with Department of Electronics, Faculty of Engineering, King Mongkut's Institute of Technology, Ladkrabang, Bangkok 10520, Thailand., E-mail: kosal_th@yahoo.com and kkyuttan@kmitl.ac.th

[3] The author is with School of Information and Telecommunication Engineering, Tokai University, 2-3-23, Takanawa, Minato-ku, Tokyo 108-8619, Japan., E-mail: kondo@keyaki.cc.u-tokai.ac.jp

for smoothing and decomposing the shape boundaries into multi-scale levels. At each scale level, then, the TAR image is computed from each three consecutive and equally apart point on the shape boundary and the corresponding Maxima-Minima lines are obtained. The matching of TAR image is based on the peaks and location of the concavity maxima in images. This scheme shows that, for the same shape, both the MTAR image and CSS image describe concavities along the contour but measure in different way. CSS method measures the curvature as the contour is smoothed by the Gaussian kernel at different scales. On the other hand, each MTAR image describes the location of the concavities using different triangle side length at a specific wavelet-smoothed scale level. For testing on the MPEG-7 dataset, the results show that MTAR image outperform CSS images based on the precision-recall curve.

N. Alajlan et al. [7] have developed a multi-scale approach for 2D closed shape matching and retrieval. In their algorithm, TAR is utilized in order to derive the multi-scale representation for 2D closed boundary shapes. Then, this triangle area normalization is made locally per scale, which is employed in the matching via dynamic programming (DP). The DP algorithm (called dynamic space warping DSW) is employed to find the best alignment between two shape representations. For the MPEG-7 CE-shape-1 database retrieval test, this method achieves high retrieval accuracy of 85.03% without corporation of the global parameters (circularity, eccentricity, aspect ratio) while combining with the global parameters, the retrieval efficiency is of 87.23%. The author also demonstrates that TAR provides useful information about shape feature such as the convexity and concavity at each boundary point. Moreover, it is robust to affine invariant and against noise and moderate amount of deformations.

M.S. Drew et al. [8] have introduced the Eigen-CSS search for shape retrieval. A new feature vector for shape representation has been created and called the marginal sum feature vector which is composed of row-sum and column-sum of the raw CSS image. Then, the PCA (called as Eigen-CSS) is used in the matching stage.

B. Wang and J.A. Bangham [9] have presented an enhanced principal component descriptor (EPCD) for shape based image retrieval. The authors have claimed that this descriptor outperforms the other descriptors including Fourier, Wavelet, and CSS descriptor.

3. THE PROPOSED METHOD

The diagram of the proposed technique for shape matching and retrieval is depicted in Fig. 1. In our algorithm, we have proposed a new multi-resolution technique to decompose shape boundary into multi-scale level, called Barycenter contour (BcC) decomposition, as detailed in section 4.2. Then, the SEA at each scale level of BcC is computed to represent shape. Mathematically, the shape is represented as 2D matrix whose column and row represent the scale level of BcC and the location index, respectively. After that, Discrete Fourier Transform (DFT) is computed for the SEA at each level to be invariant to starting point selection. In the matching stage, two frequently used classification techniques for face recognition system are utilized as classifier. They are PCA and FDA, called the Eigen Barycenter Contour (EBcC) and Fisher Barycenter Contour (FBcC) respectively in this paper. Finally, the Normalized Cross Correlation (NCC) is considered for similarity measure which is different for both conventional techniques, PCA and FDA, using Euclidian distance. This technique gives higher retrieval performance than all the published algorithms tested on the MPEG-7 database CE-1 and the Kimia's database.

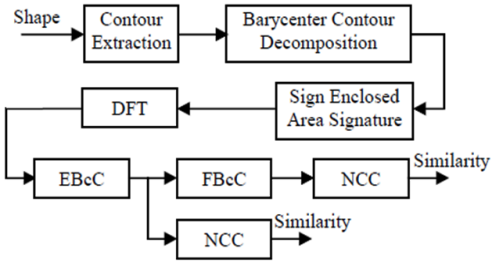

Fig.1: *The Diagram of Our Algorithm*

4. FEATURE EXTRACTION

In order to compute the shape representation, the features are extracted from the segmented shapes by performing three steps as follows:

4.1 Boundary Extraction

The shape boundary is extracted from the binary image by using one of the conventional techniques, for example chain code [10] and then presented into 1-D sequences of $x(k)$ and $y(k)$. The contour sequences are re-sampled into N points and shifted about its center point. The appropriate number of sampling points for the experiment is 128 points.

4.2 Barycenter Contour Decomposition

The BcC [11], defined in Eq. (1), is applied onto the shifted shape contour in order to obtain the different scale levels of shape boundary.

In geometry, Barycenter of a set of coordinate points is the average of this set of coordinate points. Based on this concept, the shape boundary can be decomposed into different scale levels of BcC in which the first level have been adopted from [12] and is determined from the coordinates of Barycenter of triangle composed of $(0,0)$, (x_i, y_i), and (x_{i+1}, y_{i+1}) as

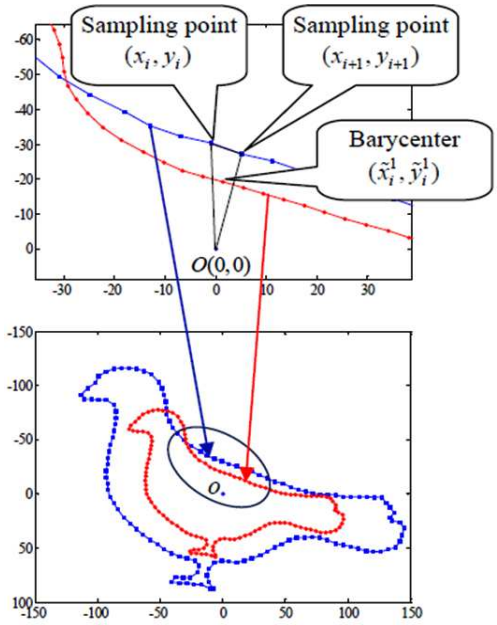

Fig.2: *The Barycenter Contour of Bird Contour at the First Level.*

depicted in Fig. 2. The second level is determined from the coordinates of Barycenter of points $(0,0)$, (x_i, y_i), (x_{i+1}, y_{i+1}), and (x_{i+2}, y_{i+2}) as depicted in Fig. 3. Just follow this process; thus, the next level is created by adding one adjacent point more to the previous level. Mathematically, if $(\tilde{x}_i, \tilde{y}_i)$ is a coordinate of Barycenter contour where $i \in \langle 1, N \rangle$, it is computed as:

$$BcC(i,m) = \begin{cases} \tilde{x}_i^m = \frac{x_i + x_{i+1} + x_{i+2} + \ldots + x_{i+m}}{m+2} \\ \tilde{y}_i^m = \frac{y_i + y_{i+1} + y_{i+2} + \ldots + y_{i+m}}{m+2} \end{cases} \quad (1)$$

where (x_i, y_i) is coordinate of shifted point; $(\tilde{x}_i, \tilde{y}_i)$ is coordinate of Barycenter point; and m is level of BcC.

Fig. 4 shows the example of Barycenter contour decomposition of bird's and device9's contour into different scale levels.

From Fig. 5, we found that level 125 is a reverse and scale version of level 1. Thus, they look very similar and the choice of the number of scale level of BcC is constrained by the implied periodicity of the closed boundary and the scale coefficient. More specifically, for a closed contour of N points:

$$BcC(i,m) = \begin{cases} -\frac{N-m}{m+2}.BcC(i+m+1, N-2-m), & \text{if } m = 1, \ldots, \lfloor \frac{N-2}{2} \rfloor \\ \frac{1}{N}\left(x_{i+N-1}, y_{i+N-1}\right), & \text{if } m = N-2 \\ 0, & \text{if } m = N-1 \\ \frac{1}{N+2}\left(x_i, y_i\right), & \text{if } m = N \end{cases} \quad (2)$$

where $\lfloor \frac{N-2}{2} \rfloor$ is the floor value of $\frac{N-2}{2}$ and the limit value of BcC. The first line in Eq. (2) shows

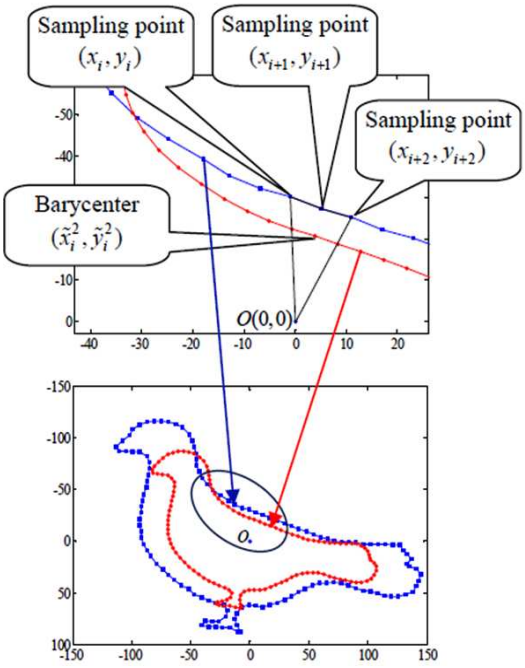

Fig.3: *The Barycenter Contour of Bird Contour at the Second Level.*

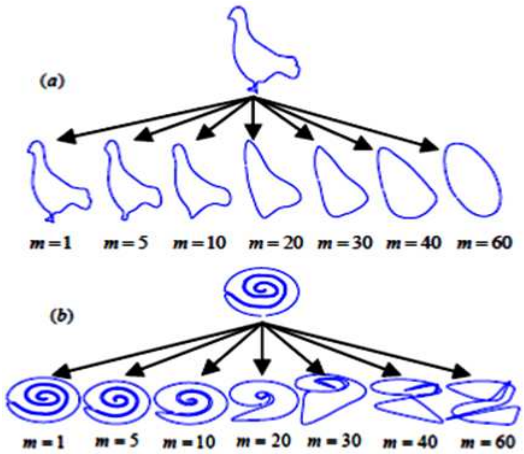

Fig.4: *Example of the BcC Decomposition of (a) Bird's and (b) Device9's Contour at Level 1, 5, 10, 20, 30, 40, and 60.*

the symmetry property including the scale version of BcC versus the level of BcC m. Also, at $m = N-1$, there is only one point of BcC, i.e., at point $(0,0)$.

Affine Transformation: The general affine transform is mathematically defined by:

$$\begin{cases} x_a = ax + by + e \\ y_a = cx + dy + f \end{cases} \quad (3)$$

From Eq. (3), we can write in a matrix form as follows:

$$\begin{bmatrix} x_a \\ y_a \\ 1 \end{bmatrix} = \begin{bmatrix} a & b & e \\ c & d & f \\ 0 & 0 & 1 \end{bmatrix} \begin{bmatrix} x \\ y \\ 1 \end{bmatrix} \quad (4)$$

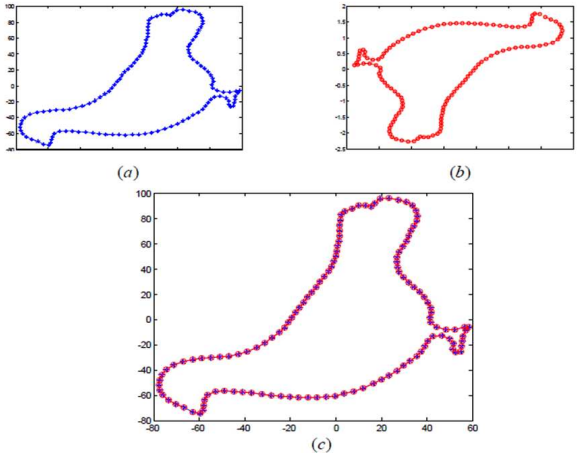

Fig.5: *The BcC of Bird Contour (a) at Level 1; (b) at Level 125; (c) A Normalization of Both Levels in Both Horizontal and Vertical Axes Where Level 125 is plotted in Reverse Direction.*

where (x, y) is the pixel coordinates of given image; (x_a, y_a) is the pixel coordinates of the distorted version of given image under general affine transformation. Translation is represented by e and f while scale, rotation, and shear are reflected in the remaining four parameters a, b, c, d.

Property: If $BcC_a(i,m) = (\tilde{x}^m_{a,i}, \tilde{y}^m_{a,i})$ is the transformed version of the $BcC(i,m) = (\tilde{x}^m_i, \tilde{y}^m_i)$ under general affine transformation, there is a one-to-one correspondence between $BcC(i,m)$ and $BcC_a(i,m)$.

Proof: From Eq. (1), the affine version of BcC is written as:

$$\begin{bmatrix} \tilde{x}^m_{a,i} \\ \tilde{y}^m_{a,i} \\ 1 \end{bmatrix} = \frac{1}{m+2} \begin{bmatrix} x_{a,i} & x_{a,i+1} & x_{a,i+2} & \dots & x_{a,i+m} \\ y_{a,i} & y_{a,i+1} & y_{a,i+2} & \dots & y_{a,i+m} \\ 1 & 1 & 1 & \dots & 1 \end{bmatrix} \begin{bmatrix} 1 \\ 1 \\ 1 \\ \vdots \\ 1 \end{bmatrix} \quad (5)$$

By Eq. (4), we can write:

$$\begin{bmatrix} x_{a,i} & x_{a,i+1} & x_{a,i+2} & \dots & x_{a,i+m} \\ y_{a,i} & y_{a,i+1} & y_{a,i+2} & \dots & y_{a,i+m} \\ 1 & 1 & 1 & \dots & 1 \end{bmatrix} = \begin{bmatrix} a & b & e \\ c & d & f \\ 0 & 0 & 1 \end{bmatrix} \begin{bmatrix} x_i & x_{i+1} & x_{i+2} & \dots & x_{i+m} \\ y_i & y_{i+1} & y_{i+2} & \dots & y_{i+m} \\ 1 & 1 & 1 & \dots & 1 \end{bmatrix} \quad (6)$$

By substituting Eq. (6) into Eq. (5), thus, we get:

$$\begin{bmatrix} \tilde{x}^m_{a,i} \\ \tilde{y}^m_{a,i} \\ 1 \end{bmatrix} = \frac{1}{m+2} \begin{bmatrix} a & b & e \\ c & d & f \\ 0 & 0 & 1 \end{bmatrix} \begin{bmatrix} x_i & x_{i+1} & x_{i+2} & \dots & x_{i+m} \\ y_i & y_{i+1} & y_{i+2} & \dots & y_{i+m} \\ 1 & 1 & 1 & \dots & 1 \end{bmatrix} \begin{bmatrix} 1 \\ 1 \\ 1 \\ \vdots \\ 1 \end{bmatrix} \quad (7)$$

Then, we have

$$\begin{bmatrix} \tilde{x}^m_{a,i} \\ \tilde{y}^m_{a,i} \\ 1 \end{bmatrix} = \begin{bmatrix} a & b & e \\ c & d & f \\ 0 & 0 & 1 \end{bmatrix} \begin{bmatrix} \tilde{x}^m_i \\ \tilde{y}^m_i \\ 1 \end{bmatrix} \quad (8)$$

By Eq. (8), we can conclude that BcC decomposition technique is affected by the same affine distortion when the shape is subjected by the affine transformation.

4.3 Shape Signature

The computation of the signed enclosed area signature at each scale level of BcC is taken into account as given in Eq. (9) and these features are presented into 3D format as the shape representation as shown in Fig. 6 where x is represented the sampling point location; y is represented the level of BcC; and z is represented the value of SEA and its DFT coefficients.

$$SEA(i,m) = \frac{1}{2}\left(\tilde{x}^m_i.\tilde{y}^m_{i+1} - \tilde{x}^m_{i+1}.\tilde{y}^m_i\right) \quad (9)$$

The shape signatures are further transformed by the Discrete Fourier Transforms (DFT) in order to be invariant to starting point selection. Then, all the DFT coefficients at each scale level are normalized by dividing with their corresponding DC component coefficients. Finally, they are concatenated into single feature vector as a new shape representation.

5. SHAPE MATCHING

In this section, we examine two classification techniques, the Eigen Barycenter Contour (EBcC) and the Fisher Barycenter Contour, for 2D shape classification.

Let $\{x_1, x_2, \dots, x_{Ns}\}$ be a set of column vectors of the shape representations taking value in n-dimensional space and suppose that each shape representation belongs to one of C classes $\{X_1, X_2, \dots, X_C\}$.

5.1 Eigen Barycenter Contour

The total covariance matrix Cov can be formed by:

$$Cov = \frac{1}{Ns}\sum_{j=1}^{Ns}(x_j - \mu)(x_j - \mu)^T \quad (10)$$

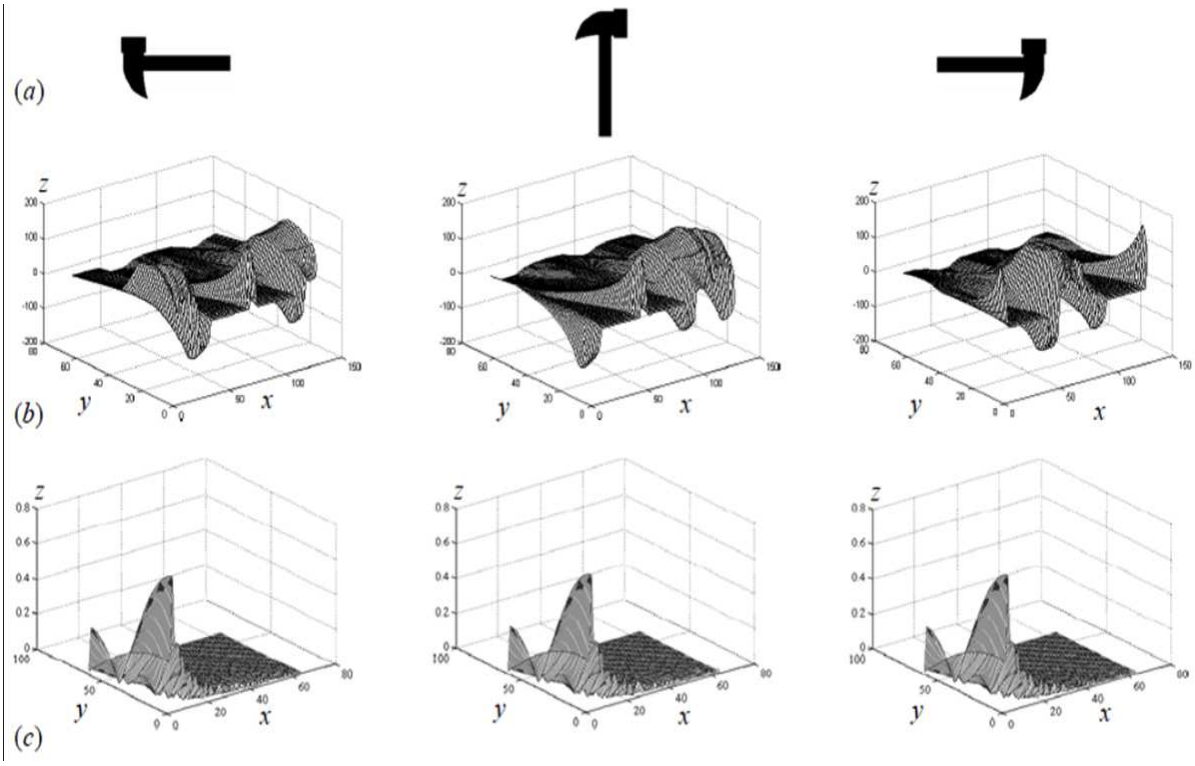

Fig.6: *(a) The Shape Silhouette, Its 90º Rotation and Its Reflection Transformation; (b) The Corresponding of SEA at All Levels of BcC as 3D Plot; (c) DFT Coefficients of SEA at All Levels of BcC as 3D Plot.*

where $\mu = \frac{1}{Ns}\sum_{j=1}^{Ns} x_j$ is the mean of all training sample sets.

Let $Q = [x_1 - \mu, x_2 - \mu, \ldots, x_{Ns} - \mu]$, so the total covariance can be expressed as follows:

$$Cov = \frac{1}{Ns} QQ^T \tag{11}$$

The objective is to find the projection axes which are the eigenvectors of the total covariance Cov. The direct finding of the eigenvectors of Cov is quite expensive computation and consumes much time. To avoid the time-consuming calculation, the singular value decomposition (SVD) technique is applied. The results from SVD are the required eigenvector $U = [u_1, u_2, u_3, \ldots, u_{Ns}]$ of Cov corresponding to the eigenvalue $\lambda_1 \geq \lambda_2 \geq \lambda_3 \geq \ldots \geq \lambda_{Ns}$.

The optimum eigenvector U_{opt} is chosen corresponding to the r largest eigenvalues where the index value r is calculated as the minimum index value of the ratio below:

$$\frac{\lambda_1 + \lambda_2 + \lambda_3 + \ldots + \lambda_r}{\lambda_1 + \lambda_2 + \lambda_3 + \ldots + \lambda_r + \ldots + \lambda_{Ns}} \geq 0.95 \tag{12}$$

Then we can obtain the j^{th} projected feature y_j from the sample x_j onto the optimum eigenvector U_{opt}:

$$y_j = U_{opt}^T (x_j - \mu) \tag{13}$$

5.2 Fisher Barycenter Contour

This method is similar to the EBcC above for dimensionality reduction by finding the optimum projection axes. The difference between the algorithms is that the eigenvectors are found by the separated matrix derived from Fisher's linear discriminant function instead of the covariance matrix. The separated matrices are the between-class scatter matrix S_B and the within-class scatter matrix S_W.

Let the between-class scatter matrix be defined as:

$$S_B = \sum_{c=1}^{C} (\mu_c - \mu)(\mu_c - \mu)^T \tag{14}$$

and the within-class scatter matrix be defined as

$$S_W = \sum_{c=1}^{C} \sum_{x_j \in X_c} (x_j - \mu_c)(x_j - \mu_c)^T \tag{15}$$

where μ_c is the mean shape representation of class X_c.

The objective is to find the optimum projection axes W_{opt} which maximizes the Fisher's ratio below:

$$J(W) = \frac{W^T S_B W}{W^T S_W W} \tag{16}$$

The solution of finding the maximum value of the Fisher's ratio is the eigenvectors of the matrix $S_W^{-1} S_B$.

Due to very expensive computation of directly finding the eigenvector from $S_W^{-1} S_B$ matrix with too large dimensional space, the result of the projected vectors from EBcC are applied to FBcC. So the eigenvectors from $S_{W(EBcC)}^{-1} S_{B(EBcC)}$ are obtained.

The top eigenvectors are selected corresponding to the $(C-1)$ largest eigenvalues of that matrix. A new projected feature z_j of the given feature x_j is computed as follows:

$$z_j = W_{opt}^T U_{opt}^T (x_j - \mu) \tag{17}$$

5.3 Similarity measure

The similarity between the unknown shape (query shape) $s_{unknown}$ and all shapes in the database s_j is measured by the normalized cross correlation value computed as follows:

$$\frac{s_{unknown}.s_j}{\|s_{unknown}\|\|s_j\|} \tag{18}$$

Then, these values are ranked in decreasing order in which the most similar shape corresponds to the highest value of the normalized cross correlation.

6. EXPERIMENT AND RESULTS

The performance of our algorithm is demonstrated using three different databases, the affine shape database, the MPEG-7 CE-shape-1 part B and the Kimia's database. For the shape matching and retrieval test, all shapes in the database are used as the test query.

The retrieval performances of our method are assessed using the precision-recall curves, where the precision value at a certain recall is the average of the precision value of all database shapes at that recall. The precision and recall can be defined by:

$$\text{Precision} = \frac{\text{Number of retrieved relevant shape}}{\text{Total number of retrieved shape}} \tag{19}$$

$$\text{Recall} = \frac{\text{Number of retrieved relevant shape}}{\text{Total number of relevant shape}} \tag{20}$$

6.1 Affine Shape Database

The affine invariant shape database [2, 11] consists of 40 categories of shapes chosen from MPEG-7 contour shape database CE-1. Each category has 14 different distorted shapes including the original shape. So there are in total 560 affine distorted shapes in this database. The sample shape in each class and the sample of affine distorted shape for class butterfly is shown in Fig. 7 and Fig. 8, respectively.

The retrieval performance is assessed by the precision-recall curve as depicted in Fig. 9. We found that the FBcC method outperforms the EBcC method for both cases. For the square of SEA signature in frequency domain have been done better than the SEA signature in frequency domain classified by FBcC method, but in contrast with EBcC method.

Fig.7: *The Sample Shape in Each Class of the Affine Shape Database.*

Fig.8: *Sample of Affine Distorted Shape of Class Butterfly*

6.2 MPEG-7 Database CE-Shape-1

The MPEG-7 CE-shape-1 database has been widely used for shape matching and retrieval. It consists of 1400 images classified into 70 classes and contains a mixture of natural and artificial objects under various rigid and non-rigid deformations. The sample shape of each class in MPEG-7 database is shown in Fig. 10.

The retrieval performance is assessed by the precision-recall curve as depicted in Fig. 11. We found that the FBcC method outperforms the EBcC method.

Additionally, we use the standard test called Bullseye test for the evaluation in which each shape are used as the test query. Retrieval is counted as correct if it is in the same class as the query. The number of correct retrievals in the top of 40 ranks is counted, including the self-match (which corresponds to the first rank). Retrieval rate for each method is reported as a ratio of the number of correct retrievals to the maximum possible number of correct retrievals, i.e. 2800 (1400 shapes * 20 correct retrievals). We have compared our results with the published results by the MPEG-7 database. Table 1 lists the Bullseye rate of some exiting techniques such as the Accurate Retrieval based on Phase (WARP) [13], shape similarity measure based on correspondence of Visual Parts (VP) [14], Curve Edit Distance (CED) [15], Curvature Scale Space (CSS) [16], Beam Angle Statistics (BAS) [17], Multi-scale Convexity Concavity representation (MCC) [18], In-

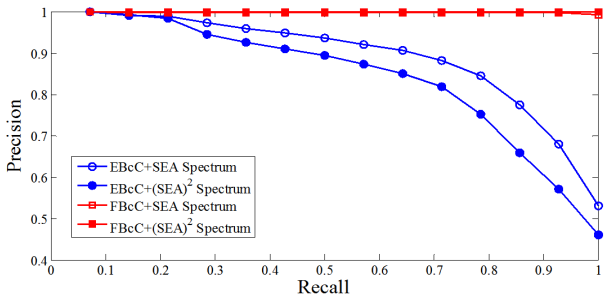

Fig.9: *The PR Curve of EBcC and FBcC Methods Tested for the Affine Shape Database.*

Fig.10: *The Sample Shape in Each Class of the MPEG-7 Database CE-Shape-1 Part B.*

ner Distance Shape Context(IDSC+DP) [19], symbolic representation [20], Triangle area representation with dynamic programming (DWS+Global) [7], Hierarchical deformable shape tree [21], and Contour flexibility [22]. All the published techniques in Table 1, the best result are reported in [22] using contour flexibility with the retrieval rate of 89.31%.

For our methods, they achieve the retrieval rate of 66.50% and 89.60% when matched by EBcC and FBcC methods, respectively. As stated early, in [6], the author have improved the performance of shape retrieval by combining with global parameters (circularity, eccentricity, aspect ratio) while our method have improved the performance by using the spectrum of squared signal of the SEA signature. In this case, they achieve the retrieval rates of 72.42% and 98.62%, respectively, when classified by EBcC and FBcC methods. We found that our FBcC method gives high retrieval performance over all published methods except EBcC method but its results are acceptable. Fig. 12 depicts the retrieval rate of each class for the MPEG-7 CE-shape-1 database. The retrieval rates of shapes in some classes are lower than the others such as hat, cup, Device9, and Device6. However, the retrieval accuracies of those classes are more than 50% in which the retrieval rate of class

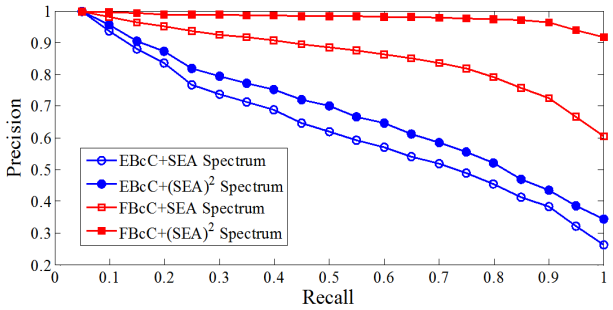

Fig.11: *The PR Curve of EBcC and FBcC Methods Tested for the MPEG-7 Shape Database.*

Table 1: *Comparison of the Bullseye Test for Different Algorithms on the MPEG-7 database*

Methods	Retrieval Accuracy (%)
WARP [13]	58.50
VP [14]	76.45
CED [15]	78.17
CSS [16]	81.12
BAS [17]	82.37
MCC [18]	84.93
IDSC + DP [19]	85.40
Symbolic Representation [20]	85.92
DSW + Global [7]	87.23
Shape tree [21]	87.70
Contour Flexibility [22]	89.31
EBcC + SEA Spectrum	**66.50**
EBcC + (SEA)^2 Spectrum	**72.42**
FBcC + SEA Spectrum	**89.60**
FBcC + (SEA)^2 Spectrum	**98.62**

'hat' is the lowest one, around 73%.

6.3 Kimia's Database

This database consists of 99 shapes from nine categories in which most of shapes are partially occluded. All the shapes in this database are shown in Fig. 13.

The precision-recall curve in Fig. 14 shows that the retrieval performance using the FBcC technique is better than that using the EBcC technique for both representations. A comparison of performances between different algorithms is summarized in Table 2, showing the correct retrievals from the top 10 closet match. Notice that the maximum number of correctness for each category is 99. We found that the EBcC method can retrieve in 10 cases of 735 shapes which is low performance comparing with other algorithms. However, the FBcC method achieves a good result of 100% when the spectrum of the squared SEA signature is utilized as the representation.

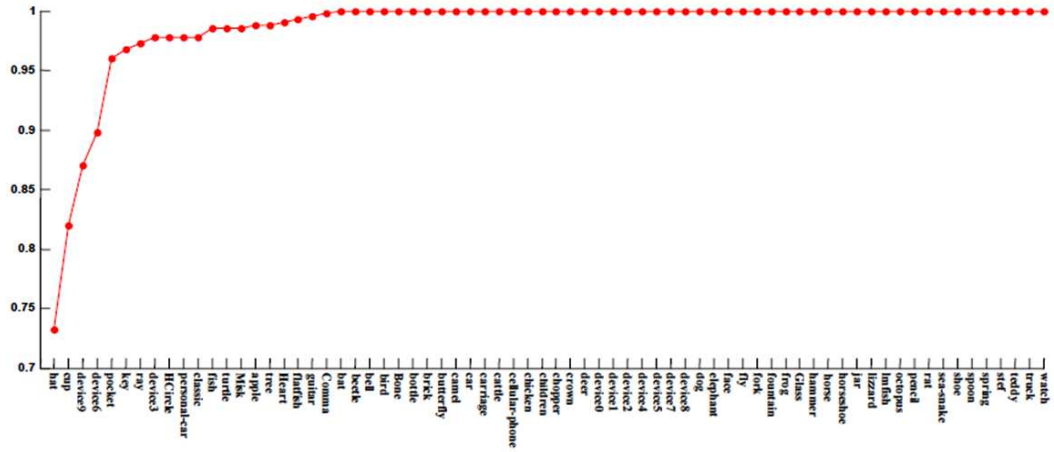

Fig.12: *The Retrieval Accuracy for Each Class of the MPEG-7 Database Using FBcC+(SEA)^2 Spectrum*

Table 2: *Comparison of the Retrieval Rate for Different Algorithms on Kimias Database*

Methods	1^{st}	2^{nd}	3^{rd}	4^{th}	5^{th}	6^{th}	7^{th}	8^{th}	9^{th}	10^{th}	**Total**
Shape context [23]	97	91	88	85	84	77	75	66	56	37	756
Shock graph [15]	99	99	99	98	98	97	96	95	93	82	956
MDS+SC+DP [19]	99	98	98	98	97	99	97	96	97	85	964
DSW+Global [7]	99	99	99	98	98	97	98	95	96	94	956
Symbolic representation [20]	99	99	99	98	99	98	98	95	96	94	975
EBcC + SEA Spectrum	**99**	**94**	**87**	**82**	**76**	**73**	**65**	**60**	**54**	**45**	**735**
EBcC + (SEA)^2 Spectrum	**99**	**94**	**94**	**92**	**82**	**84**	**82**	**77**	**67**	**57**	**828**
FBcC + SEA Spectrum	**99**	**99**	**99**	**99**	**97**	**98**	**98**	**95**	**97**	**94**	**975**
FBcC + (SEA)^2 Spectrum	**99**	**99**	**99**	**99**	**99**	**99**	**99**	**99**	**99**	**99**	**990**

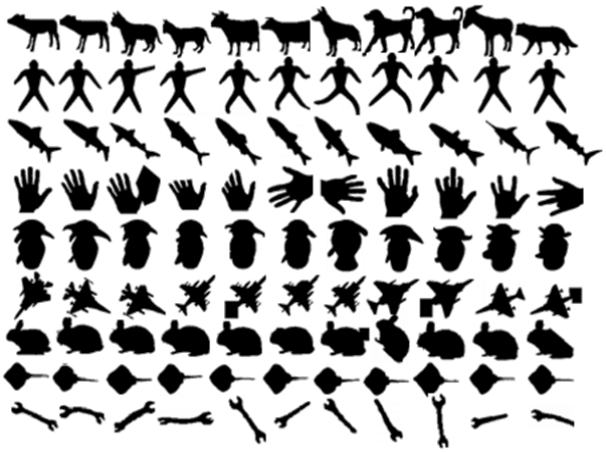

Fig.13: *All Shapes in the Kimia's Database.*

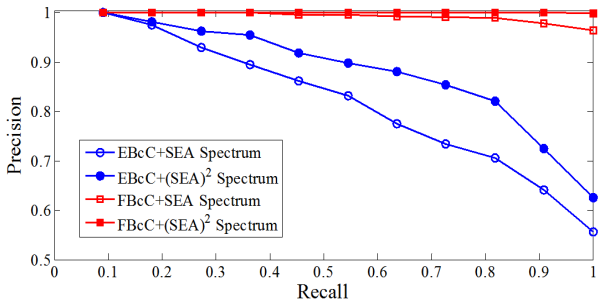

Fig.14: *The PR Curve of EBcC and FBcC Methods Tested for the Kimia's Database.*

7. CONCLUSION

We present the technique for 2D closed boundary shape matching and retrieval using Eigen Barycenter Contour (EBcC) and Fisher Barycenter Contour (FBcC).

The proposed algorithm is robust to affine transformation including translation, rotation, scale and shear. In our algorithm, the BcC decomposition has been employed for decomposing the shape into multiscale levels in order to reduce the noise and small boundary distortion.

Because of the high dimensionality of data, two classification techniques, EBcC and FBcC, are used for dimensionality reduction. The results show that the retrieval accuracy experimented by EBcC technique is acceptable over three databases. While using FBcC technique, it does not only outperform the EBcC method but also achieves high retrieval rate over the existing methods, based on the Bullseye test, which is tested on the two well-known database, the MPEG-7 database and the Kimia's database. Furthermore, the performance of our algorithm has been

improved using only the spectrum of the squared SEA signature as the shape representation which is different from the algorithm in [7] using the global parameters (circularity, eccentricity, aspect ratio) to improve their performance.

References

[1] S. Lambert, E. de Leau, and L. Vuurpijl, "Using pen-based outlines for object-based annotation and image-based queries," *International Conference on Visual Information and Information Systems.,* June 1999, pp. 585-592.

[2] K. Thourn and Y. Kitjaidure, "Multi-View Shape Recognition Based on Principal Component Analysis," *International Conference on Advanced Computer Control.,* Jan. 2009, pp. 265-269.

[3] D. Zhang and G. Lu, "Review of shape representation and description techniques," *Pattern Recognition 37(1).,* 2004, pp. 1-19.

[4] P.M. Belhumeur, J.P. Haspanha, and D.J. Kriegman, "Eigenfaces vs. Fisherfaces: Recognition Using Class Specific Linear Projection," *IEEE Trans. on Pattern Analysis and Machine Intelligence.,* Vol. 19, No. 7, July 1997, pp. 711-720.

[5] Marios Savvides, B.V.K. Vijaya Kumar and P.K. Khosla, "Eigenphases vs. Eigenfaces," *Proceedings of the 17th International Conference on Pattern Recognition.,* 2004, pp. 810-813.

[6] I.El Rube, N. Alajlan, M. Kamel, M. Ahmed and G. Freeman, "Efficient Multiscale Shape-Based Representation and Retrieval," *International Conference on Image Analysis and Recognition.,* September 2005, pp. 415-422.

[7] N. Alajlan, I. El Rube, M.S. Kamel, and G. Freeman, "Shape retrieval using triangle-area representation and dynamic space warping," *Pattern Recognition 40.,* 2007, pp. 1911-1920.

[8] M.S. Drew, T.K. Lee, and A. Rova, "Shape Retrieval with Eigen-CSS Search," *Image and Vision Computing 27.,* 2009, pp. 748-755.

[9] B. Wang and J.A. Bangham, "PCA Based Shape Descriptors for Shape Retrieval and the Evaluations," *International Conference on Computational Intelligence and Security.,* 2006, pp. 1401-1406.

[10] L.da.F. Costa and R.M. Cesar Jr, Shape Analysis and Classification: Theory and Practice, CRC Press LLC, 2001.

[11] K. Thourn and Y. Kitjaidure, and S. Kondo, "Affine Invariant Shape Recognition Based on Multi-Level of Barycenter contour," *International Symposium on Communication and Information Technologies.,* October 2008, pp. 145-149.

[12] P. Thumwarin and T. Matsuura, "On-line writer recognition for Thai based on velocity of Barycenter of pen-point movement," *International Conference on Image Processing.,* 2004, pp. 889-892.

[13] I. Bartolini, P. Ciaccia, and M. Patella, "WARP: Accurate Retrieval of Shapes Using Phase of Fourier Descriptors and Time Warping Distance," *IEEE Trans. on Pattern Analysis and Machine Intelligence.,* vol 27, No. 1,January 2005, pp. 142-147.

[14] L.J. Latecki and R. Lakamper, "Shape Similarity Measure Based on Correspondence of Visual Parts," *IEEE Trans. on Pattern Analysis and Machine Intelligence.,* vol. 22, No. 10, October 2000, pp. 1185-1190.

[15] T. Sebastian, P. Klein, and B. Kimia, "On Aligning Curves," *IEEE Trans. on Pattern Analysis and Machine Intelligence.,* vol. 25, No. 1, January 2003, pp. 116-125.

[16] F. Mokhtarian and M. Bober, Curvature Scale Space Representation: Theory, Applications, and MPEG-7 Standardization, Kluwer Academic Publishers, 2003.

[17] N. Arica and F. Vural, "BAS: A Perceptual Shape Descriptor Based on the Beam Angle Statistics," *Pattern Recognition Letter.,* 2003, pp. 1627-1639.

[18] T. Adamek and N.E. O'Connor, "A Multiscale Representation Method for Nonrigid Shapes with a Single Closed Contour," *IEEE Trans. on Circuits System and Video Technology.,* 2004, pp. 742-753.

[19] H. Ling, and D. Jacobs, "Shape Classification Using Inner-Distance," *IEEE Trans. on Pattern Analysis and Machine Intelligence.,* vol. 29, No. 2, February 2007, pp. 286-299.

[20] M.R. Darili and V. Torre, "Robust Symbolic Representation for Shape Recognition and Retrieval," *Pattern Recognition 41.,* 2008, pp. 1782-1798.

[21] P.F. Felzenszwalb and J.D. Schwartz, "Hierarchical Matching of Deformable Shapes," *IEEE Conference on Computer Vision and Pattern Recognition.,* 2007, pp. 1-8.

[22] C. Xu, J. Liu and X. Tang, "2D Shape Matching by Contour Flexibility," *IEEE Trans. On Pattern Analysis and Machine Intelligence.,* Vol. 31, No. 1, January 2009, pp. 180-186.

[23] S. Belongie, J. Malik, and J. Puzicha, "Shape Matching and Object Recognition Using Shape Context," *IEEE Trans. on Pattern Analysis and Machine Intelligence.,* vol. 24, No. 4, April 2002, pp. 509-522.

Kosorl Thourn was born in Kandal, Cambodia, on August 28, 1985. He received his B.Eng degree in electrical engineering from the Institute of Technology of Cambodia (ITC), in June 2007. In October 2007, he was awarded the AUN SEED-Net scholarship supported by JICA to continue his master degree at the Department of Electronics, King Mongkut's Institute of Technology, Ladkrabang (KMITL), Bangkok, Thailand. His research interests include shape classification, pattern recognition and digital image processing.

Yuttana Kitjaidure was born in Bangkok, Thailand in 1964. He received B.Eng and M.Eng degrees from King Mongkuts Institute of Technology Ladkrabang, Thailand in 1986 and 1989, respectively and the Ph.D degree in Electrical and Electronics Engineering from the Imperial college, London University, England in 1998. He currently works at King Mongkut's Institute of Technology Ladkrabang, Thailand. His current research interests are in the fields of computational Intelligence applied in image and signal processing also in control systems.

Shozo Kondo received the B.E. degree form the Department of Electrical Engineering, Waseda Univertsity, Japan in 1968 and M.E. and Ph.D from Graduate School of Electrical Engineering, Waseda University, Japan in 1970 and 1973, respectively. He was an Associative Professor at school of Engineering, Tokai University in 1974 and became a Professor in 1986. He was a visiting professor in INRIA, France from 1992 to 1993. He is currently a professor at school of Information Science and Technology, Tokai University. His current research interests are in image processing using wavelet transform and biometrics. He is a member of IEEE, IPSJ, and IEICE.